Eur. Phys. J. C 54, 591–599 (2008)
DOI 10.1140/epjc/s10052-008-0553-2

THE EUROPEAN PHYSICAL JOURNAL C

Regular Article – Theoretical Physics

# Exclusive $B \to K_1 \ell^+ \ell^-$ decay in model with single universal extra dimension

I. Ahmed[1,a], M.A. Paracha[1], M.J. Aslam[2]

[1] Department of Physics and National Centre for Physics, Quaid-i-Azam University, Islamabad, Pakistan
[2] Department of Physics, COMSATS Institute of Information Technology, Chak Shahzad Campus, Islamabad, Pakistan

Received: 11 December 2007 / Revised version: 30 January 2008 /
Published online: 28 February 2008 – 

**Abstract.** Decay rate and forward–backward asymmetries in $B \to K_1 \ell^+ \ell^-$, where $K_1$ is the axial vector meson, are calculated in the universal extra dimension (UED) model. The dependence of these physical quantities on the compactification radius $R$, the only unknown parameter in UED model, is studied, and it is shown that the zero of the forward–backward asymmetry is sensitive to the UED model; therefore they can be a very useful tool to establish new physics predicted by the UED model. This work is briefly extended to $B \to K^* l^+ l^-$.

## 1 Introduction

The flavor-changing neutral-current (FCNC) transitions $b \to s$ provide potentially stringent tests of the standard model (SM) in flavor physics and are not allowed at tree level but are induced by the Glashow–Iliopoulos–Miani (GIM) amplitudes [1] at the loop level in the SM. In addition, they are also suppressed in the SM due to their dependence on the weak mixing angles of the quark-flavor rotation matrix – the Cabibbo–Kobayashi–Maskawa (CKM) matrix [2, 3]. These two circumstances make the FCNC decays relatively rare and hence important for the study of physics beyond the SM, commonly known as new physics.

The experimental observation of inclusive [4] and exclusive [5, 6] decays, $B \to X_s \gamma$ and $B \to K^* \gamma$, has prompted a lot of theoretical interest in rare $B$ meson decays. Though the inclusive decays are theoretically better understood but are extremely difficult to measure in a hadron machine such as the LHC, which is the only collider, except for a super-$B$ factory, which could provide enough luminosity for a precise study of the decay distribution of such rare processes. In contrast, the exclusive decays are easy to detect experimentally but are challenging to calculate theoretically; the difficulty lies in describing the hadronic structure, which provides the main uncertainty in the predictions of exclusive rare decays. In exclusive $B \to K, K^*$ decays the long-distance effects in the meson transition amplitude of the effective Hamiltonian are encoded in the meson transition form factors, which are scalar functions of the square of the momentum transfer and are model dependent quantities. Many exclusive $B \to K\,(K^*)\,\ell^+\ell^-$[16–34], $B \to \phi \ell^+ \ell^-$ [41], $B \to \gamma \ell^+ \ell^-$ [35–40], and $B \to \ell^+ \ell^-$ [42–48] processes based on $b \to s\,(d)\,\ell^+\ell^-$ have been studied in the literature and many frameworks have been applied to the description of meson transition form factors, like constituent quark models, QCD sum rules, lattice QCD, approaches based on heavy quark symmetry, and analytical constraints.

Rare $B$ decay modes also provide important ways to look for physics beyond the SM. There are various extensions of the SM in the literature, but the models with extra dimensions are of viable interest as they provide a unified framework for gravity and other interactions. In this way they give some hints of the hierarchy problem and a connection with string theory. Among different models of extra dimensions, which differ from one another depending on the number of extra dimensions, the most interesting ones are the scenarios with universal extra dimensions. In these UED models all the SM fields are allowed to propagate in the extra dimensions and compactification of an extra dimension leads to the appearance of Kaluza–Klein (KK) partners of the SM fields in the four-dimensional description of higher dimensional theory, together with KK modes without corresponding SM partners. The Appelquist, Cheng and Dobrescu (ACD) model [49] with one universal extra dimension is very attractive, because it has only one free parameter with respect to the SM and that is the inverse of the compactification radius $R$ [50–52].

By analyzing the signature of the extra dimensions in the different processes, one can get bounds on the size of the extra dimensions, which are different in different models. These bounds are accessible for the processes already known at the particle accelerators or within the reach of planned future facilities. In the case of UED these bounds are more severe, and constraints from Tevatron run I allow one to put the bound $1/R \geq 300\,\text{GeV}$ [50–52].

Rare $B$ decays can also be used to constrain the ACD scenario, and in this regard Buras and collaborators have

[a] e-mail: ishtiaq@ncp.edu.pk

already done some work. In addition to the effective Hamiltonian they have calculated for $b$–$s$ decays and also investigated the impact of UED on $B^0$–$\bar{B}^0$ mixing as well as on the CKM unitarity triangle [53–55]. Due to availability of precise data on the decays $B \to K\,(K^*)\,\ell^+\ell^-$, Colangelo et al. studied these decays in ACD model by calculating the branching ratio and forward backward asymmetry [50]. We will study the rare semileptonic decay modes $B \to K_1 \ell^+ \ell^-$ on the same footing as $B \to K^* \ell^+ \ell^-$, because both are induced by the same quark level transitions, i.e. $b \to s \ell^+ \ell^-$. We compare results of the forward–backward asymmetry for $B \to K^* l^+ l^-$ using our form factors with those obtained by Colangelo et al. [50–52]. The comparison shows a clear distinction as shown in Fig. 4. These decays may provide us a step forward towards the study of the existence of new physics beyond the SM and therefore deserve serious attention, both theoretically and experimentally.

The paper is organized as follows. In Sect. 2 we will briefly introduce the ACD model. Section 3 deals with the study of the effective Hamiltonian and the corresponding matrix elements for $B \to K_1 \ell^+ \ell^-$ decay. Now the new physics becomes manifest in these decays in two different ways: either through new operators in the effective Hamiltonian, which are absent in the SM, or through new contributions to the Wilson coefficients [41]. In ACD no new operator appears at tree level and therefore the new physics comes only through the Wilson coefficients, which have been calculated in the literature [54, 55], and we will summarize them in the same section. Finally, in Sect. 4 we will calculate the decay rate and forward–backward asymmetry and summarize our results.

## 2 ACD Model

In our usual universe we have 3 spatial +1 temporal dimensions, and if an extra dimension exists and is compactified, fields living in all dimensions would manifest themselves in the $3+1$ space by the appearance of Kaluza–Klein excitations. The most pertinent question is whether ordinary fields propagate or not in all extra dimensions. One obvious possibility is the propagation of gravity in the whole ordinary plus extra dimensional universe, the "bulk". Contrary to this there are the models with universal extra dimensions in which all the fields propagate in all available dimensions [49], and the Appelquist, Cheng and Dobrescu model belongs to one of the UED scenarios [50–52].

This model is the minimal extension of the SM in $4+\delta$ dimensions, and in the literature the simple case $\delta = 1$ is considered [50–52]. The topology for this extra dimension is the orbifold $S^1/Z_2$, and the coordinate $x_5 = y$ runs from 0 to $2\pi R$, where $R$ is the compactification radius. The Kaluza–Klein mode expansions of the fields are determined from the boundary conditions at the two fixed points $y = 0$ and $y = \pi R$ on the orbifold. Under the parity transformation $P_5$, $y \to -y$, the fields may be even or odd. Even fields have corresponding ones in the four-dimensional SM, and their zero mode in the KK mode expansion can be interpreted as the ordinary SM field. The odd fields do not have corresponding ones in the SM and therefore do not have a zero mode in the KK expansion.

The significant features of the ACD model are

i) the compactification radius $R$ is the only free parameter with respect to the SM;
ii) no tree level contribution of KK modes in low-energy processes (at scale $\mu \ll 1/R$) and no production of a single KK excitation in ordinary particle interactions is a consequence of the conservation of KK parity.

The detailed description of the ACD model is provided in [54]; here, we summarize the main features of its construction from [50–52].

*Gauge group.* As the ACD model is the minimal extension of the SM, the gauge bosons associated with the gauge group $\mathrm{SU}(2)_\mathrm{L} \times \mathrm{U}(1)_Y$ are $W_i^a$ $(a = 1, 2, 3,\ i = 0, 1, 2, 3, 5)$ and $B_i$; the gauge couplings are $\hat{g}_2 = g_2\sqrt{2\pi R}$ and $\hat{g}' = g'\sqrt{2\pi R}$ (the hat on the coupling constant refers to the extra dimension). The charged bosons are $W_i^\pm = \frac{1}{\sqrt{2}}\left(W_i^1 \mp W_i^2\right)$ and the mixings of $W_i^3$ and $B_i$ give rise to the fields $Z_i$ and $A_i$ as they do in the SM. The relations for the mixing angles are

$$c_\mathrm{W} = \cos\theta_\mathrm{W} = \frac{\hat{g}_2}{\sqrt{\hat{g}_2^2 + \hat{g}'^2}} \quad c_\mathrm{W} = \sin\theta_\mathrm{W} = \frac{\hat{g}'}{\sqrt{\hat{g}_2^2 + \hat{g}'^2}}\,. \tag{1}$$

The Weinberg angle remains the same as in the SM, due to the relationship between the five- and four-dimensional constants. The gluons, which are the gauge bosons associated to $\mathrm{SU}(3)_C$, are $G_i^a\,(x, y)$ $(a = 1, \ldots, 8)$.

*Higgs sector and mixing between Higgs fields and gauge bosons.* The Higgs doublet can be written as

$$\phi = \begin{pmatrix} \mathrm{i}\chi^+ \\ \frac{1}{\sqrt{2}}\left(\psi - \mathrm{i}\chi^3\right) \end{pmatrix}, \tag{2}$$

with $\chi^\pm = \frac{1}{\sqrt{2}}\left(\chi^1 \mp \chi^2\right)$. Now only the field $\psi$ has a zero mode, and we assign a vacuum expectation value $\hat{v}$ to such a mode, so that $\psi \to \hat{v} + H$. $H$ is the SM Higgs field, and the relation between the expectation values in five and four dimensions is $\hat{v} = v/\sqrt{2\pi R}$.

The Goldstone fields $G^0_{(n)}$ and $G^\pm_{(n)}$ arise due to the mixing of the charged $W^\pm_{5(n)}$ and $\chi^\pm_{(n)}$, as well as the neutral fields $Z_{5(n)}$. These Goldstone modes are then used to give masses to the $W^{\pm\mu}_{(n)}$ and $Z^\mu_{(n)}$; $a^0_{(n)}$ and $a^\pm_{(n)}$ are new physical scalars.

*Yukawa terms.* In the SM, Yukawa coupling of the Higgs field to the fermion provides the fermion mass terms. The diagonalization of such terms leads to the introduction of the CKM matrix. In order to have chiral fermions in the ACD model, the left- and right-handed components of the given spinor cannot be simultaneously even under $P_5$. This makes the ACD model the minimal flavor violation model, since there are no new operators beyond those present in the SM and no new phase beyond the CKM phase and

the unitarity triangle remains the same as in the SM [54]. In order to have 4D mass eigenstates of higher KK levels, a further mixing is introduced among the left-handed doublet and right-handed singlet of each flavor $f$. The mixing angle is such that $\tan\left(2\alpha_{f(n)}\right) = \frac{m_f}{n/R}\,(n \geq 1)$, giving a mass $m_{f(n)} = \sqrt{m_f^2 + \frac{n^2}{R^2}}$, so that it is negligible for all flavors except for the top [50–52].

Integrating over the fifth dimension $y$ gives the four-dimensional Lagrangian

$$\mathcal{L}_4\,(x) = \int_0^{2\pi R} \mathcal{L}_5\,(x,y)\;, \tag{3}$$

which describes

(i) zero modes corresponding to the SM fields;
(ii) their massive KK excitations;
(iii) KK excitations without zero modes that do not correspond to any field in the SM – the Feynman rules used in the further calculations are given in [54].

## 3 Effective Hamiltonian

At quark level the decay $B \to K_1 \ell^+ \ell^-$ is the same as $B \to K^* \ell^+ \ell^-$, as discussed by Ali et al. [16], i.e. $b \to s \ell^+ \ell^-$, and it can be described by an effective Hamiltonian obtained by integrating out the top quark and the $W^\pm$ bosons:

$$H_{\rm eff} = -4\frac{G_{\rm F}}{\sqrt{2}} V_{tb} V_{ts}^* \sum_{i=1}^{10} C_i(\mu) O_i(\mu)\,, \tag{4}$$

where the $O_i$ are four local quark operators and the $\dot{C}_i$ are Wilson coefficients calculated in the naive dimensional regularization (NDR) scheme [56].

One can write the above Hamiltonian in the following free quark decay amplitude:

$$\begin{aligned}\mathcal{M}(b \to s\ell^+\ell^-) &= \frac{G_{\rm F}\alpha}{\sqrt{2}\pi} V_{tb} V_{ts}^* \\ &\times \Big\{ C_9^{\rm eff}\left[\bar{s}\gamma_\mu L b\right]\left[\bar{\ell}\gamma^\mu \ell\right] + C_{10}\left[\bar{s}\gamma_\mu L b\right]\left[\bar{\ell}\gamma^\mu\gamma^5\ell\right] \\ &- 2\hat{m}_b C_7^{\rm eff}\left[\bar{s}{\rm i}\sigma_{\mu\nu}\frac{\hat{q}^\nu}{\hat{s}} R b\right]\left[\bar{\ell}\gamma^\mu\ell\right]\Big\}\end{aligned} \tag{5}$$

with $L/R \equiv \frac{(1\mp\gamma_5)}{2}$; we have $s = q^2$, which is just the momentum transfer from heavy to light meson. The amplitude given in (5) contains long-distance effects encoded in the form factors and short-distance effects that are hidden in the Wilson coefficients. These Wilson coefficients have been computed at next-to-next leading order (NNLO) in the SM [57–64]. Specifically for exclusive decays, the effective coefficient $C_9^{\rm eff}$ can be written as

$$C_9^{\rm eff} = C_9 + Y\,(\hat{s})\;, \tag{6}$$

where the perturbatively calculated result of $Y\,(\hat{s})$ is [56]

$$\begin{aligned}Y_{\rm pert}\,(\hat{s}) &= g\,(\hat{m}_c,\hat{s})\,(3C_1 + C_2 + 3C_3 + C_4 + 3C_5 + C_6) \\ &- \frac{1}{2} g\,(1,\hat{s})\,(4C_3 + 4C_4 + 3C_5 + C_6) \\ &- \frac{1}{2} g\,(0,\hat{s})\,(C_3 + 3C_4) \\ &+ \frac{2}{9}\,(3C_3 + C_4 + 3C_5 + C_6)\,.\end{aligned} \tag{7}$$

Here the hat denotes the normalization in terms of the mass of the $B$ meson. For the explicit expressions of the $g$ and numerical values of the Wilson coefficients appearing in (7) we refer to [56].

In the ACD model the new physics comes through the Wilson coefficients. Buras et al. have computed the above coefficients at NLO in the ACD model including the effects of the KK modes [54, 55]; we use these results to study $B \to K_1 \ell^+ \ell^-$ decay. As has already been mentioned, the ACD model is the minimal extension of the SM with only one extra dimension, and it has no extra operator other than the SM; therefore, the whole contribution from all the KK states is in the Wilson coefficients, i.e. now they depend on the additional ACD parameter, the inverse of the compactification radius $R$. At large value of $1/R$ the SM phenomenology should be recovered, since the new states, being more and more massive, decoupled from the low-energy theory. Our objective is to calculate the decay rate and the forward–backward asymmetry for $B \to K_1 \ell^+ \ell^-$ using the lower bound on $1/R$ provided by Colangelo et al. for $B \to K^* \ell^+ \ell^-$ decay [50–52].

In the ACD model, the Wilson coefficients are modified and they contain the contributions from new particles, which are not present in the SM and which come as intermediate states in penguin and box diagrams. Thus, these coefficients can be expressed in terms of the functions $F\,(x_t, 1/R)$, $x_t = \frac{m_t^2}{M_W^2}$, which generalize the corresponding SM function $F_0\,(x_t)$ according to

$$F\,(x_t, 1/R) = F_0\,(x_t) + \sum_{n=1}^{\infty} F_n\,(x_t, x_n)\;, \tag{8}$$

with $x_n = \frac{m_n^2}{M_W^2}$ and $m_n = \frac{n}{R}$ [50–52]. The relevant diagrams are $Z^0$ penguins, $\gamma$ penguins, gluon penguins, $\gamma$ magnetic penguins, chromomagnetic penguins, and the corresponding functions are $C\,(x_t, 1/R)$, $D\,(x_t, 1/R)$, $E\,(x_t, 1/R)$, $D'\,(x_t, 1/R)$ and $E'\,(x_t, 1/R)$, respectively. These functions can be found in [54, 55], but to make this paper self-contained, we collect here the formulae needed for our analysis.

In place of $C_7$, one defines an effective coefficient $C_7^{(0)\rm eff}$, which is renormalization scheme independent [65]:

$$\begin{aligned}C_7^{(0)\rm eff}(\mu_b) &= \eta^{\frac{16}{23}} C_7^{(0)}\,(\mu_w) + \frac{8}{3}\left(\eta^{\frac{14}{23}} - \eta^{\frac{16}{23}}\right) C_8^{(0)}(\mu_w) \\ &+ C_2^{(0)}(\mu_w) \sum_{i=1}^{8} h_i \eta^{\alpha_i}\,,\end{aligned} \tag{9}$$

where $\eta = \frac{\alpha_s(\mu_w)}{\alpha_s(\mu_b)}$, and

$$C_2^{(0)}(\mu_w) = 1\,, \quad C_7^{(0)}(\mu_w) = -\frac{1}{2}D'\left(x_t, \frac{1}{R}\right),$$
$$C_8^{(0)}(\mu_w) = -\frac{1}{2}E'\left(x_t, \frac{1}{R}\right); \tag{10}$$

the superscript (0) is for the leading log approximation. Furthermore

$$\alpha_1 = \frac{14}{23}\,, \quad \alpha_2 = \frac{16}{23}\,, \quad \alpha_3 = \frac{6}{23}\,, \quad \alpha_4 = -\frac{12}{23}\,,$$
$$\alpha_5 = 0.4086\,, \quad \alpha_6 = -0.4230\,, \quad \alpha_7 = -0.8994\,,$$
$$\alpha_8 = -0.1456\,, \quad h_1 = 2.996\,, \quad h_2 = -1.0880\,, \quad h_3 = -\frac{3}{7}\,,$$
$$h_4 = -\frac{1}{14}\,, \quad h_5 = -0.649\,, \quad h_6 = -0.0380\,,$$
$$h_7 = -0.0185\,, \quad h_8 = -0.0057\,. \tag{11}$$

The functions $D'$ and $E'$ are given by (11) with

$$D_0'(x_t) = -\frac{\left(8x_t^3 + 5x_t^2 - 7x_t\right)}{12(1-x_t)^3} + \frac{x_t^2(2-3x_t)}{2(1-x_t)^4}\ln x_t\,, \tag{12}$$

$$E_0'(x_t) = -\frac{x_t\left(x_t^2 - 5x_t - 2\right)}{4(1-x_t)^3} + \frac{3x_t^2}{2(1-x_t)^4}\ln x_t\,, \tag{13}$$

$$D_n'(x_t, x_n) = \frac{x_t\begin{pmatrix} -37 + 44x_t + 17x_t^2 \\ +6x_n^2\left(10 - 9x_t + 3x_t^2\right) \\ -3x_n\left(21 - 54x_t + 17x_t^2\right)\end{pmatrix}}{36(x_t-1)^3} + \frac{x_n(2 - 7x_n + 3x_n^2)}{6}\ln\frac{x_n}{1+x_n} - \frac{\begin{pmatrix}(-2 + x_n + 3x_t) \\ \times\left(x_t + 3x_t^2 + x_n^2(3+x_t) - x_n\right) \\ \times(1 + (-10 + x_t)x_t)\end{pmatrix}}{6(x_t-1)^4}\ln\frac{x_n + x_t}{1+x_n} \tag{14}$$

$$E_n'(x_t, x_n) = \frac{x_t\begin{pmatrix} -17 - 8x_t + x_t^2 - 3x_n\left(21 - 6x_t + x_t^2\right) \\ -6x_n^2\left(10 - 9x_t + 3x_t^2\right)\end{pmatrix}}{12(x_t-1)^3} - \frac{1}{2}x_n(1+x_n)(-1+3x_n)\ln\frac{x_n}{1+x_n} + \frac{(1+x_n)\begin{pmatrix} x_t + 3x_t^2 + x_n^2(3+x_t) \\ -x_n\left(1 + (-10 + x_t)x_t\right)\end{pmatrix}}{2(x_t-1)^4} \times \ln\frac{x_n + x_t}{1+x_n}\,. \tag{15}$$

Following [54] one gets the expressions for the sum over $n$:

$$\sum_{n=1}^{\infty} D_n'(x_t, x_n) = -\frac{x_t(-37 + x_t(44 + 17x_t))}{72(x_t-1)^3} + \frac{\pi M_w R}{2}\left[\int_0^1 \mathrm{d}y \frac{2y^{\frac{1}{2}} + 7y^{\frac{3}{2}} + 3y^{\frac{5}{2}}}{6}\right] \times \coth(\pi M_w R\sqrt{y}) + \frac{(-2+x_t)x_t(1+3x_t)}{6(x_t-1)^4}J\left(R, -\frac{1}{2}\right) - \frac{1}{6(x_t-1)^4}[x_t(1+3x_t) - (-2+3x_t) \times (1 + (-10+x_t)x_t)]J\left(R, \frac{1}{2}\right) + \frac{1}{6(x_t-1)^4}[(-2+3x_t)(3+x_t) - (1 + (-10+x_t)x_t)]J\left(R, \frac{3}{2}\right) - \frac{(3+x_t)}{6(x_t-1)^4}J\left(R, \frac{5}{2}\right)\Bigg], \tag{16}$$

$$\sum_{n=1}^{\infty} E_n'(x_t, x_n) = -\frac{x_t(-17 + (-8 + x_t)x_t)}{24(x_t-1)^3} + \frac{\pi M_w R}{2}\left[\int_0^1 \mathrm{d}y(y^{\frac{1}{2}} + 2y^{\frac{3}{2}} - 3y^{\frac{5}{2}}) \times \coth(\pi M_w R\sqrt{y})\right] - \frac{x_t(1+3x_t)}{(x_t-1)^4}J\left(R, -\frac{1}{2}\right) + \frac{1}{(x_t-1)^4}[x_t(1+3x_t) - (1 + (-10+x_t)x_t)]J\left(R, \frac{1}{2}\right) - \frac{1}{(x_t-1)^4}[(3+x_t) - (1 + (-10+x_t)x_t)]J\left(R, \frac{3}{2}\right) + \frac{(3+x_t)}{(x_t-1)^4}J\left(R, \frac{5}{2}\right)\Bigg], \tag{17}$$

where

$$J(R, \alpha) = \int_0^1 \mathrm{d}y y^{\alpha}\left[\coth(\pi M_w R\sqrt{y}) - x_t^{1+\alpha}\coth(\pi m_t R\sqrt{y})\right]. \tag{18}$$

For $C_9$, in the ACD model and in the NDR scheme one has

$$C_9(\mu) = P_0^{\mathrm{NDR}} + \frac{Y(x_t, \frac{1}{R})}{\sin^2\theta_{\mathrm{W}}} - 4Z\left(x_t, \frac{1}{R}\right) + P_E E\left(x_t, \frac{1}{R}\right) \tag{19}$$

where $P_0^{\mathrm{NDR}} = 2.60 \pm 0.25$ [56] and the last term is numerically negligible. Besides

$$Y\left(x_t, \frac{1}{R}\right) = Y_0(x_t) + \sum_{n=1}^{\infty} C_n(x_t, x_n)$$
$$Z\left(x_t, \frac{1}{R}\right) = Z_0(x_t) + \sum_{n=1}^{\infty} C_n(x_t, x_n) \tag{20}$$

with

$$Y_0(x_t) = \frac{x_t}{8}\left[\frac{x_t-4}{x_t-1} + \frac{3x_t}{(x_t-1)^2}\ln x_t\right]$$
$$Z_0(x_t) = \frac{18x_t^4 - 163x_t^3 + 259x_t^2 - 108x_t}{144(x_t-1)^3} + \left[\frac{32x_t^4 - 38x_t^3 + 15x_t^2 - 18x_t}{72(x_t-1)^4} - \frac{1}{9}\right]\ln x_t \tag{21}$$

$$C_n(x_t, x_n) = \frac{x_t}{8(x_t-1)^2} \times \left[x_t^2 - 8x_t + 7 + (3 + 3x_t + 7x_n - x_t x_n)\ln\frac{x_t + x_n}{1+x_n}\right] \tag{22}$$

and

$$\sum_{n=1}^{\infty} C_n(x_t, x_n) = \frac{x_t(7-x_t)}{16(x_t-1)} - \frac{\pi M_w R x_t}{16(x_t-1)^2} \times \left[3(1+x_t)J\left(R, -\frac{1}{2}\right) + (x_t-7)J\left(R, \frac{1}{2}\right)\right]. \tag{23}$$

$C_{10}$ is $\mu$ independent and is given by

$$C_{10} = -\frac{Y(x_t, \frac{1}{R})}{\sin^2\theta_w}. \tag{24}$$

The normalization scale is fixed at $\mu = \mu_b \simeq 5$ GeV.

Wilson coefficients give the short-distance effects, whereas the long-distance effects involve the matrix elements of the operators in (5) between the $B$ and $K_1$ mesons. Using the standard parameterization in terms of the form factors we have [66]

$$\langle K_1(k,\varepsilon)|V_\mu|B(p)\rangle = \mathrm{i}\varepsilon_\mu^*(M_B + M_{K_1})V_1(s) - (p+k)_\mu(\varepsilon^*\cdot q)\frac{V_2(s)}{M_B + M_{K_1}} - q_\mu(\varepsilon\cdot q)\frac{2M_{K_1}}{s}[V_3(s) - V_0(s)], \tag{25}$$

$$\langle K_1(k,\varepsilon)|A_\mu|B(p)\rangle = \frac{2\mathrm{i}\epsilon_{\mu\nu\alpha\beta}}{M_B + M_{K_1}}\varepsilon^{*\nu}p^\alpha k^\beta A(s), \tag{26}$$

where $V_\mu = \bar{s}\gamma_\mu b$ and $A_\mu = \bar{s}\gamma_\mu\gamma_5 b$ are the vector and axial vector currents respectively, and $\varepsilon_\mu^*$ is the polarization vector for the final state axial vector meson.

The relationship between different form factors, which also ensures that there is no kinematical singularity in the matrix element at $s = 0$, is

$$V_3(s) = \frac{M_B + M_{K_1}}{2M_{K_1}}V_1(s) - \frac{M_B - M_{K_1}}{2M_{K_1}}V_2(s), \tag{27}$$
$$V_3(0) = V_0(0). \tag{28}$$

In addition to the above form factors there are also some penguin form factors, which are

$$\langle K_1(k,\varepsilon)|\bar{s}\mathrm{i}\sigma_{\mu\nu}q^\nu b|B(p)\rangle = \left[\left(M_B^2 - M_{K_1}^2\right)\varepsilon_\mu - (\varepsilon\cdot q)(p+k)_\mu\right]F_2(s) + (\varepsilon^*\cdot q)\left[q_\mu - \frac{s}{M_B^2 - M_{K_1}^2}(p+k)_\mu\right]F_3(s), \tag{29}$$

$$\langle K_1(k,\varepsilon)|\bar{s}\mathrm{i}\sigma_{\mu\nu}q^\nu\gamma_5 b|B(p)\rangle = -\mathrm{i}\epsilon_{\mu\nu\alpha\beta}\varepsilon^{*\nu}p^\alpha k^\beta F_1(s), \tag{30}$$

with $F_1(0) = 2F_2(0)$.

Form factors are non-perturbative quantities and are scalar functions of the square of the momentum transfer. Different models are used to calculate these form factors. The form factors we use here in the analysis of physical variables like decay rate and forward–backward asymmetry have been calculated using Ward identities. The detailed calculations and their expressions are given in [66] and can be summarized as follows:

$$A(s) = \frac{A(0)}{(1 - s/M_B^2)(1 - s/M_B'^2)},$$
$$V_1(s) = \frac{V_1(0)}{\left(1 - s/M_{B_A^*}^2\right)\left(1 - s/M_{B_A^*}'^2\right)}\left(1 - \frac{s}{M_B^2 - M_{K_1}^2}\right), \tag{31}$$
$$V_2(s) = \frac{\tilde{V}_2(0)}{\left(1 - s/M_{B_A^*}^2\right)\left(1 - s/M_{B_A^*}'^2\right)} - \frac{2M_{K_1}}{M_B - M_{K_1}}\frac{V_0(0)}{(1 - s/M_B^2)(1 - s/M_B'^2)},$$

with

$$A(0) = -(0.52 \pm 0.05),$$
$$V_1(0) = -(0.24 \pm 0.02),$$
$$\tilde{V}_2(0) = -(0.39 \pm 0.03). \tag{32}$$

The corresponding values for $B \to K^*$ form factors at $s = 0$ are given by

$$V(0) = (0.29 \pm 0.04),$$
$$A_1(0) = (0.23 \pm 0.03), \tag{33}$$
$$\tilde{A}_2(0) = (0.33 \pm 0.05).$$

## 4 Decay distribution and forward–backward asymmetry

In this section we define the decay rate distribution, which we shall use for the phenomenological analysis. Following the notation of [16] we can write, from (5),

$$\mathcal{M} = \frac{G_\mathrm{F}\alpha}{2\sqrt{2}\pi}V_{tb}V_{ts}^* m_B\left[\mathcal{T}_\mu^1\left(\bar{l}\gamma^\mu l\right) + \mathcal{T}_\mu^2\left(\bar{l}\gamma^\mu\gamma^5 l\right)\right], \tag{34}$$

where

$$\mathcal{T}_\mu^1 = A\left(\hat{s}\right)\varepsilon_{\mu\rho\alpha\beta}\epsilon^{*\rho}\hat{p}_B^\alpha\hat{p}_{K_1}^\beta - \mathrm{i}B\left(\hat{s}\right)\epsilon_\mu^* + \mathrm{i}C\left(\hat{s}\right)\left(\epsilon^*\cdot\hat{p}_B\right)\hat{p}_{h\mu} + \mathrm{i}D\left(\hat{s}\right)\left(\epsilon^*\cdot\hat{p}_B\right)\hat{q}_\mu\,, \tag{35}$$

$$\mathcal{T}_\mu^2 = E\left(\hat{s}\right)\varepsilon_{\mu\rho\alpha\beta}\epsilon^{*\rho}\hat{p}_B^\alpha\hat{p}_{K_1}^\beta - \mathrm{i}F\left(\hat{s}\right)\epsilon_\mu^* + \mathrm{i}G\left(\hat{s}\right)\left(\epsilon^*\cdot\hat{p}_B\right)\hat{p}_{h\mu} + \mathrm{i}H\left(\hat{s}\right)\left(\epsilon^*\cdot\hat{p}_B\right)\hat{q}_\mu\,. \tag{36}$$

The definitions of the different momenta involved are in [16], where the auxiliary functions are

$$\begin{aligned}
A(\hat{s}) &= -\frac{2A(\hat{s})}{1+\hat{M}_{K_1}}C_9^{\mathrm{eff}}(\hat{s}) + \frac{2\hat{m}_b}{\hat{s}}C_7^{\mathrm{eff}}F_1(\hat{s})\,,\\
B(\hat{s}) &= \left(1+\hat{M}_{K_1}\right)\left[C_9^{\mathrm{eff}}(\hat{s})V_1(\hat{s}) + \frac{2\hat{m}_b}{\hat{s}}C_7^{\mathrm{eff}}\left(1-\hat{M}_{K_1}\right)F_2(\hat{s})\right]\,,\\
C\left(\hat{s}\right) &= \frac{1}{\left(1-\hat{M}_{K_1}^2\right)}\left\{C_9^{\mathrm{eff}}(\hat{s})V_2(\hat{s}) + 2\hat{m}_b C_7^{\mathrm{eff}} \times \left[F_3(\hat{s}) + \frac{1-\hat{M}_{K_1}^2}{\hat{s}}F_2(\hat{s})\right]\right\}\,,\\
D(\hat{s}) &= \frac{1}{\hat{s}}\left[\left(C_9^{\mathrm{eff}}(\hat{s})(1+\hat{M}_{K_1})V_1(\hat{s}) - (1-\hat{M}_{K_1})V_2(\hat{s}) - 2\hat{M}_{K_1}V_0(\hat{s})\right) - 2\hat{m}_b C_7^{\mathrm{eff}}F_3(\hat{s})\right]\,,\\
E(\hat{s}) &= -\frac{2A(\hat{s})}{1+\hat{M}_{K_1}}C_{10}\,,\\
F(\hat{s}) &= \left(1+\hat{M}_{K_1}\right)C_{10}V_1(\hat{s})\,,\\
G(\hat{s}) &= \frac{1}{1+\hat{M}_{K_1}}C_{10}V_2(\hat{s})\,,\\
H(\hat{s}) &= \frac{1}{\hat{s}}\left[C_{10}(\hat{s})(1+\hat{M}_{K_1})V_1(\hat{s}) - (1-\hat{M}_{K_1})V_2(\hat{s}) - 2\hat{M}_{K_1}V_0(\hat{s})\right]\,.
\end{aligned} \tag{37}$$

Considering the final state lepton as a muon, the branching ratio for $B \to K_1\mu^+\mu^-$ is calculated in [66], and its numerical value is

$$\mathcal{B}\left(B \to K_1\mu^+\mu^-\right) = 0.9^{+0.11}_{-0.14} \times 10^{-7}\,.$$

The above value of the branching ratio is for the case if one does not include $Y(\hat{s})$ in (7). The error in the value reflects the uncertainty from the form factors and are due to the variation of the input parameters like CKM matrix elements, the decay constant of the $B$ meson and the masses as defined in Table 1.

By including $Y(\hat{s})$ the central value of the branching ratio reduces to

$$\mathcal{B}\left(B \to K_1\mu^+\mu^-\right) = 0.72 \times 10^{-7}\,.$$

It has already been mentioned that in the ACD model there is no new operator beyond the SM and new physics will come only through the Wilson coefficients. To see this, the differential branching ratio against $\hat{s}$ is plotted in Fig. 1

**Table 1.** Default value of input parameters used in the calculation

| | |
|---|---|
| $m_{\mathrm{W}}$ | 80.41 GeV |
| $m_Z$ | 91.1867 GeV |
| $sin^2\theta_{\mathrm{W}}$ | 0.2233 |
| $m_c$ | 1.4 GeV |
| $m_{b,\mathrm{pole}}$ | $4.8 \pm 0.2$ GeV |
| $m_t$ | $173.8 \pm 5.0$ GeV |
| $\alpha_s\left(m_Z\right)$ | $0.119 \pm 0.0058$ |
| $f_B$ | $(200 \pm 30)$ MeV |
| $\lvert V_{ts}^* V_{tb}\rvert$ | 0.0385 |

using the central values of the input parameters. One can see that there is significant enhancement in the decay rate due to the KK contribution for $1/R = 200\,\mathrm{GeV}$, whereas the value is shifted towards the SM at large values of $1/R$. The enhancement is prominent in the low value of $\hat{s}$, but such effects are obscured by the uncertainties involved in different parameters like the form factors, the CKM matrix elements etc. The numerical value at these two different values of $1/R$ is

$$\mathcal{B}\left(B \to K_1\mu^+\mu^-\right) = 0.82 \times 10^{-7} \text{ for } 1/R = 200\,\mathrm{GeV}\,,$$
$$\mathcal{B}\left(B \to K_1\mu^+\mu^-\right) = 0.75 \times 10^{-7} \text{ for } 1/R = 500\,\mathrm{GeV}\,.$$

The effects of UED become clearer if we look for the FB asymmetry in the dilepton angular distribution, because it depends upon the Wilson coefficients. It is known that in the SM, due to the opposite sign of the $C_7$ and $C_9$, the forward–backward asymmetry passes from its zero position and has a very weak dependence on the form factors and uncertainties in the input parameters. The differential forward–backward asymmetry for $B \to K_1\mu^+\mu^-$ reads [16]

$$\frac{\mathrm{d}\mathcal{A}_{\mathrm{FB}}}{\mathrm{d}\hat{s}} = \frac{G_{\mathrm{F}}^2\alpha^2 m_B^5}{2^{10}\pi^5}\left|V_{ts}^*V_{tb}\right|^2\hat{s}\hat{u}\left(\hat{s}\right)\left[\mathrm{Re}\left(BE^*\right) + \mathrm{Re}\left(AF^*\right)\right]\,, \tag{38}$$

where

$$\begin{aligned}
\hat{u}\left(\hat{s}\right) &= \sqrt{\lambda\left(1 - 4\frac{\hat{m}_l^2}{\hat{s}}\right)}\\
\lambda &\equiv \lambda\left(1, \hat{m}_{K_1}^2, \hat{s}\right)\\
&= 1 + \hat{m}_{K_1}^4 + \hat{s}^2 - 2\hat{s} - 2\hat{m}_{K_1}^2\left(1+\hat{s}\right)\,.
\end{aligned} \tag{39}$$

The variable $\hat{u}$ corresponds to $\theta$, the angle between the momentum of the $B$ meson and the positively charged lepton in the dilepton c.m. system frame. In the SM the zero-point of the forward–backward asymmetry for $B \to K_1\mu^+\mu^-$ is calculated by Paracha et al. [66], and it lies at $\hat{s} = 0.16$ $\left(s = 4.46\,\mathrm{GeV}^{-2}\right)$. They have shown that due to the uncertainties in the form factors the zero position of the forward–backward asymmetry $A_{\mathrm{FB}}$ deviates slightly from the central value in the low $s$ region, whereas in the large $s$ region these deviations are highly suppressed and the zero of the forward–backward asymmetry becomes insensitive to these uncertainties; therefore, we do not include them while analyzing the above decay in the UED model.

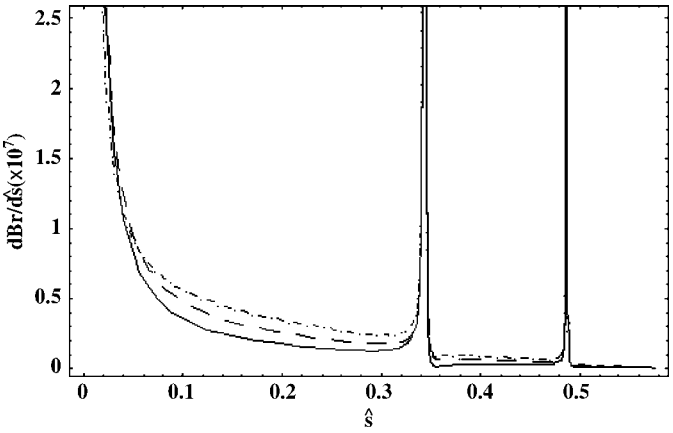


**Fig. 1.** The differential branching ratio as a function of $\hat{s}$ is plotted using the form factors defined in (31). The *solid line* denotes the SM result, the *dashed-dotted* line is for $1/R = 200$ GeV and the *dashed line* is for $1/R = 500$ GeV. All the input parameters are taken at their central values

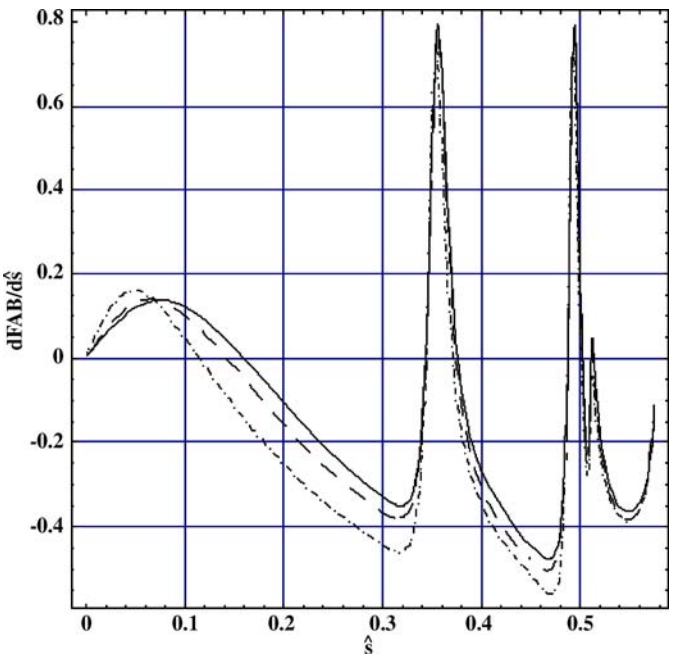


**Fig. 2.** The differential forward–backward (FB) asymmetry as a function of $\hat{s}$ is plotted using the form factors defined in (31). The *solid line* denotes the SM result, the *dashed-dotted line* is for $1/R = 200$ GeV and the *dashed line* is for $1/R = 500$ GeV. All the input parameters are taken at their central values

To see the new physics effects due to the extra dimension, the differential forward–backward asymmetry with $\hat{s}$ is plotted in Fig. 2. It can be seen that the zero position of the forward–backward asymmetry $A_{\rm FB}$ shifts towards the left in the ACD model with a single universal extra dimension and this shifting is clearer for $1/R = 200$ GeV. In the future, when we have some data on these decays, this sensitivity of the zero position to the compactification parameter will be used to constrain $1/R$.

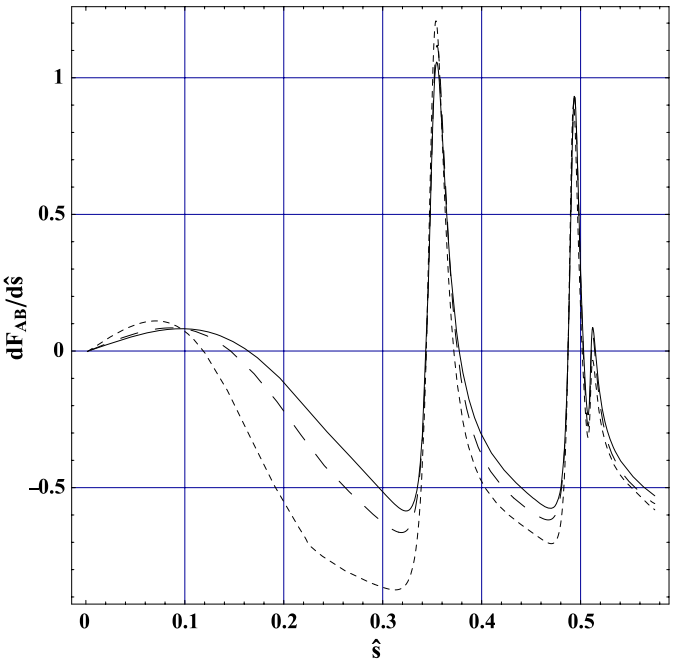


**Fig. 3.** The differential forward–backward (FB) asymmetry for $B \to K^* \ell^+ \ell^-$ as a function of $\hat{s}$ is plotted using the form factors defined in (31) with obvious replacements for $K^*$. The *solid line* denotes the SM result, the *dashed line* is for $1/R = 200$ GeV and the *long-dashed line* is for $1/R = 500$ GeV. All the input parameters are taken at their central values

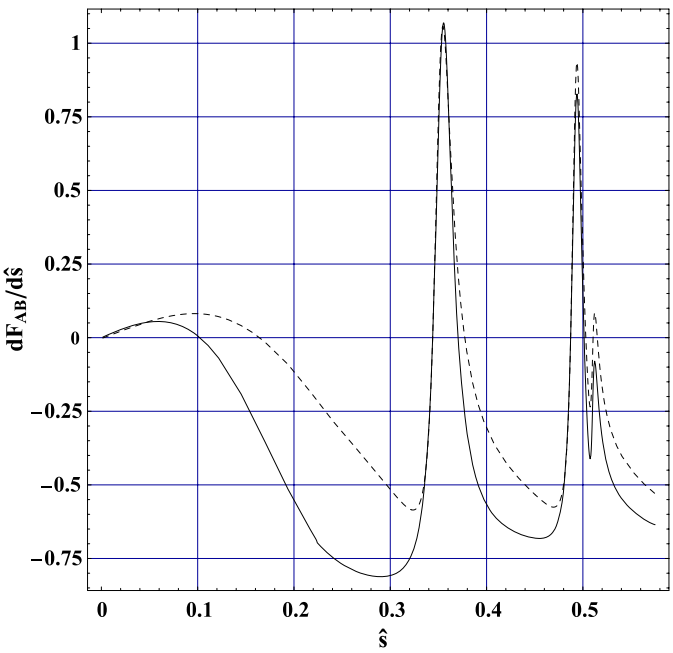


**Fig. 4.** Comparison of the differential forward–backward (FB) asymmetry for $B \to K^* l^+ l^-$ in the SM as a function of $\hat{s}$, plotted using the form factors defined in (31) versus the form factors given in Colangelo et al. [50–52]. The *solid line* denotes the Colangelo result and the *dashed line* denotes our result

The method of calculation of the form factors for $B \to K_1 \ell^+ \ell^-$ decay described in [66] can be straightforwardly used to calculate the form factors for $B \to K^* \ell^+ \ell^-$. Now after calculating these form factors for $B \to K^* \ell^+ \ell^-$ we have plotted the forward–backward asymmetry with $\hat{s}$ in Fig. 3. We believe that it provides a useful comparison, if one compares the effect of our form factors on the zero of $A_{\rm FB}$ with other ones, like in [16] and references therein. Again the zero of $A_{\rm FB}$ is shifted towards the left in the ACD model with a single universal extra dimension, and this shifting is clearer for $1/R = 200\,\text{GeV}$.

## 5 Conclusion

This paper deals with the study of the semileptonic decay $B \to K_1 \ell^+ \ell^-$ in the ACD model with a single universal extra dimension, which is a strong contender to study physics beyond the SM and has received a lot of interest in the literature. We studied the dependence of the physical observables, like the decay rate and the zero position of the forward–backward asymmetry, on the inverse of the compactification radius $1/R$. The value of the branching ratio is found to be larger than the corresponding SM value. The zero position of the FB asymmetry is very sensitive to $1/R$, and it is seen that it shifts significantly to the left. The shifting is large at $1/R = 200\,\text{GeV}$ and approaches the SM value if we increase the value of $1/R$. Future experiments, in which more data are expected, will put stringent constraints on the compactification radius and also give us some deep understanding of $B$-physics.

## References


1. S.L. Glashow, J. Iliopoulos, L. Maiani, Phys. Rev. D **2**, 1285 (1970)
2. N. Cabibbo, Phys. Rev. Lett. **10**, 531 (1963)
3. M. Kobayashi, K. Maskawa, Prog. Theor. Phys. **49**, 652 (1973)
4. M.S. Alam et al., Phys. Rev. Lett. **74**, 2885 (1995)
5. R. Ammar et al., Phys. Rev. Lett. **71**, 674 (1993)
6. CLEO CONF 96-05 (1996)
7. B. Grinstein, M.B. Wise, M.J. Savage, Nucl. Phys. B **319**, 271 (1989)
8. A. Buras, M. Munz, Phys. Rev. D **52**, 186 (1995)
9. A. Ali, T. Mannel, T. Morozumi, Phys. Lett. B **273**, 505 (1991)
10. A. Ali, Acta Phys. Pol. B **27**, 35 298 (1996)
11. A. Ali, Nucl. Instrum. Methods Phys. Res. A **384**, 8 (1996)
12. C.S. Lim, T. Morozumi, A.T. Sanda, Phys. Lett. B **218**, 343 (1989)
13. P.J. O'Donnell, H.K.K. Tung, Phys. Rev. D **43**, R2067 (1991)
14. T. Inami, C.S. Lim, Prog. Theor. Phys. **65**, 297 (1981)
15. G. Buchalla, A.J. Buras, Nucl. Phys. B **400**, 225 (1993)
16. A. Ali, P. Ball, L.T. Handoko, G. Hiller, Phys. Rev. D **61**, 074 024 (2000) [arXiv:hep-ph/9910221]
17. T.M. Aliev, M.K. Cakmak, M. Savci, Nucl. Phys. B **607**, 305 (2001) [arXiv:hep-ph/0009133]
18. T.M. Aliev, A. Ozpineci, M. Savci, C. Yuce, Phys. Rev. D **66**, 115 006 (2002) [arXiv:hep-ph/0208128]
19. T.M. Aliev, A. Ozpineci, M. Savci, Phys. Lett. B **511**, 49 (2001) [arXiv:hep-ph/0103261]
20. T.M. Aliev, M. Savci, Phys. Lett. B **481**, 275 (2000) [arXiv:hep-ph/0003188]
21. T.M. Aliev, D.A. Demir, M. Savci, Phys. Rev. D **62**, 074 016 (2000) [arXiv:hep-ph/9912525]
22. T.M. Aliev, C.S. Kim, Y.G. Kim, Phys. Rev. D **62**, 014 026 (2000) [arXiv:hep-ph/9910501]
23. T.M. Aliev, E.O. Iltan, Phys. Lett. B **451**, 175 (1999) [arXiv:hep-ph/9804458]
24. C.H. Chen, C.Q. Geng, Phys. Rev. D **66**, 034 006 (2002) [arXiv:hep-ph/0207038]
25. C.H. Chen, C.Q. Geng, Phys. Rev. D **66**, 014 007 (2002) [arXiv:hep-ph/0205306]
26. G. Erkol, G. Turan, Nucl. Phys. B **635**, 286 (2002) [arXiv:hep-ph/0204219]
27. E.O. Iltan, G. Turan, I. Turan, J. Phys. G **28**, 307 (2002) [arXiv:hep-ph/0106136]
28. T.M. Aliev, V. Bashiry, M. Savci, JHEP **0405**, 037 (2004) [arXiv:hep-ph/0403282]
29. W.J. Li, Y.B. Dai, C.S. Huang, arXiv:hep-ph/0410317
30. Q.S. Yan, C.S. Huang, W. Liao, S.H. Zhu, Phys. Rev. D **62**, 094 023 (2000) [arXiv:hep-ph/0004262]
31. S.R. Choudhury, N. Gaur, A.S. Cornell, G.C. Joshi, Phys. Rev. D **68**, 054 016 (2003) [arXiv:hep-ph/0304084]
32. S.R. Choudhury, A.S. Cornell, N. Gaur, G.C. Joshi, Phys. Rev. D **69**, 054 018 (2004) [arXiv:hep-ph/0307276]
33. A. Ali, E. Lunghi, C. Greub, G. Hiller, Phys. Rev. D **66**, 034 002 (2002) [arXiv:hep-ph/0112300]
34. F. Kruger, E. Lunghi, Phys. Rev. D **63**, 014 013 (2001) [arXiv:hep-ph/0008210]
35. S.R. Choudhury, N. Gaur, N. Mahajan, Phys. Rev. D **66**, 054 003 (2002) [arXiv:hep-ph/0203041]
36. S.R. Choudhury, N. Gaur, arXiv:hep-ph/0205076
37. S.R. Choudhury, N. Gaur, arXiv:hep-ph/0207353
38. T.M. Aliev, V. Bashiry, M. Savci, Phys. Rev. D **71**, 035 013 (2005) [arXiv:hep-ph/0411327]
39. U.O. Yilmaz, B.B. Sirvanli, G. Turan, Nucl. Phys. **692**, 249 (2004) [arXiv:hep-ph/0407006]
40. U.O. Yilmaz, B.B. Sirvanli, G. Turan, Eur. Phys. J. C **30**, 197 (2003) [arXiv:hep-ph/0304100]
41. R. Mohanta, A.K. Giri, arXiv:hep-ph/0611068
42. S.R. Choudhury, N. Gaur, Phys. Lett. B **451**, 86 (1999) [arXiv:hep-ph/9810307]
43. J.K. Mizukoshi, X. Tata, Y. Wang, Phys. Rev. D **66**, 115 003 (2002) [arXiv:hep-ph/0208078]
44. T. Ibrahim, P. Nath, Phys. Rev. D **67**, 016 005 (2003) [arXiv:hep-ph/0208142]
45. G.L. Kane, C. Kolda, J.E. Lennon, arXiv:hep-ph/0310042
46. A.J. Buras, P.H. Chankowski, J. Rosiek, L. Slawianowska, Nucl. Phys. B **659**, 3 (2003) [arXiv:hep-ph/0210145]
47. A.J. Buras, P.H. Chankowski, J. Rosiek, L. Slawianowska, Phys. Lett. B **546**, 96 (2002) [arXiv:hep-ph/0207241]
48. A. Dedes, H.K. Dreiner, U. Nierste, Phys. Rev. Lett. **87**, 251 804 (2001) [arXiv:hep-ph/0108037]
49. T. Appelquist, H.C. Cheng, B.A. Dobrescu, Phys. Rev. D **64**, 035 002 (2001)
50. P. Colangelo, F. De Fazio, R. Ferrandes, T.N. Pham, Phys. Rev. D **73**, 115 006 (2006)

51. P. Colangelo, F. De Fazio, P. Santorelli, E. Scrimieri, Phys. Rev. D **53**, 3672 (1996)
52. P. Colangelo, Phys. Rev. D **57**, 3186 (1998), Erratum
53. K. Agashe, N.G. Deshpande, G.H. Wu, Phys. Lett. B **514**, 309 (2001)
54. A.J. Buras, M. Spranger, A. Weiler, Nucl. Phys. B **660**, 225 (2003)
55. A.J. Buras, A. Poschenrieder, M. Spranger, A. Weiler, Nucl. Phys. B **678**, 455 (2004)
56. A.J. Buras et al., Nucl. Phys. B **424**, 374 (1994)
57. C. Bobeth, M. Misiak, J. Urban, Nucl. Phys. B **574**, 291 (2000)
58. H.H. Asatrian, H.M. Asatrian, C. Greub, M. Walker, Phys. Lett. B **507**, 162 (2001)
59. C. Bobeth, Phys. Rev. D **65**, 074004 (2002)
60. C. Bobeth, Phys. Rev. D **66**, 034009 (2002)
61. H.M. Asatrian, K. Bieri, C. Greub, A. Hovhannisyan, Phys. Rev. D **66**, 094013 (2002)
62. A. Ghinculov, T. Hurth, G. Isidori, Y.P. Yao, Nucl. Phys. B **648**, 254 (2003)
63. A. Ghinculov, T. Hurth, G. Isidori, Y.P. Yao, Nucl. Phys. B **685**, 351 (2004)
64. C. Bobeth, P. Gambino, M. Gorbahn, U. Haisch, JHEP **0404**, 071 (2004)
65. A.J. Buras, M. Misiak, M. Munz, S. Pokorski, Nucl. Phys. B **424**, 374 (1994)
66. M.A. Paracha, I. Ahmed, M.J. Aslam, Eur. Phys. J. C **52**, 967 (2007)